Volume 11 • Issue 1 • Spring 2007

CONTENTS

features

SPECIAL REPORT: BUSTING SCIENTIFIC MYTHS

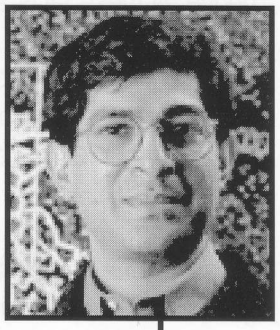

research

RESEARCH PAPERS

ectric and Magnetic Characterization of Sputtered Iron in Films and the Implications for Chromium Thin Films

Aidin Fathalizadeh*, Zoe Boekelheide**
*Department of Physics and Mathematics, **Department of Physics
University of California at Berkeley

Keywords: *Magnetron, Spectrometer, Sputtered, Thin films*

RACT: Sputtered thin films of iron are utilized in many industrial applications. As a ferromagnetic material, iron n employed along with the antiferromagnetic chromium in Fe/Cr multilayers, which exhibit giant magnetoresis-ffects (GMR). We have grown sputtered thin films of iron at various argon sputtering gas pressures, as well as for thicknesses, and studied the resistivity and magnetic characteristics of the films. Films grown at different pres-ave significantly different microstructure and stress. Films grown at higher chamber pressures exhibit higher ity and lower saturation magnetization than those deposited at lower sputtering pressures. SEM surface images, ition to quartz crystal deposition rate detector methods, indicate higher chamber pressures result in looser grains s dense films. A similar investigation for chromium thin films reveals similar changes in stress and structure, but nore drastic variation in the resistivity for different pressures, implying more than structural properties at work, ce that band effects come into play for the Cr films.

ODUCTION

ered iron is utilized in the construction of Fe/Cr multilay-ese multilayers exhibit a large change in resistivity when ve ferromagnetic iron layers, which are antiparallel in the of a magnetic field, are made parallel by an external field. gins of this giant magnetoresistance effect (GMR) has been c of much speculation. It has been suggested that some spin orbit coupling is responsible for the effect (Gurney et). To understand the GMR of multilayers, we must first end the characteristics of sputtered thin films of iron and m.

cent investigations of chromium thin films reveal drastic s in their resistivity when grown under different sputter-nber pressures (Boekelheide 2006). Previous studies sug-he larger and looser grain structure of films deposited at ressures account for the observed changes in resistivity n 1977). In the model proposed by Thornton, ejected tar-s lose energy through collisions with argon atoms on their he substrate. In such a scenario, materials of similar atom-should exhibit similar structure and, therefore, similar s in resistivity when grown under the same sputtering ns. The crystal structure and lattice constant of target s are also important, but we note that both chromium and body-centered cubic with similar lattice constants of 2.88 87 Å respectively. A closer analysis of chromium thin wever, reveals a gradual change in the spin density waves materials as sputtering pressure is adjusted, implying that ects contribute to the observed phenomenon. Hence in ng thin films of iron, with its similar atomic mass to n, we hope to understand whether structural anomalies n account for the large resistivity changes in chromium s.

his investigation, thin films of iron were deposited on sil-trates covered by amorphous silicon nitride (SiNx) using tron sputtering chamber. One investigation involved film thicknesses at a constant chamber pressure. The different sputtering gas pressures was also studied. The results of the electrical and magnetic characterization, as well as the underlying structure, of these films are presented here.

MATERIALS AND METHODS

Magnetron Sputtering Thin films of iron were deposited on 1 cm x 1 cm SiNx covered silicon substrates by means of DC magnetron sputtering in a high vacuum chamber at room temperature (Figure 1). The iron target was a disk of radius 2.5 cm with a purity of 99.95%. Upon loading the substrates into the sputtering chamber, the chamber was pumped down to a base pressure of less than 5x10-8 Torr. Such high vacuum conditions reduce the impurities in the deposited thin films.

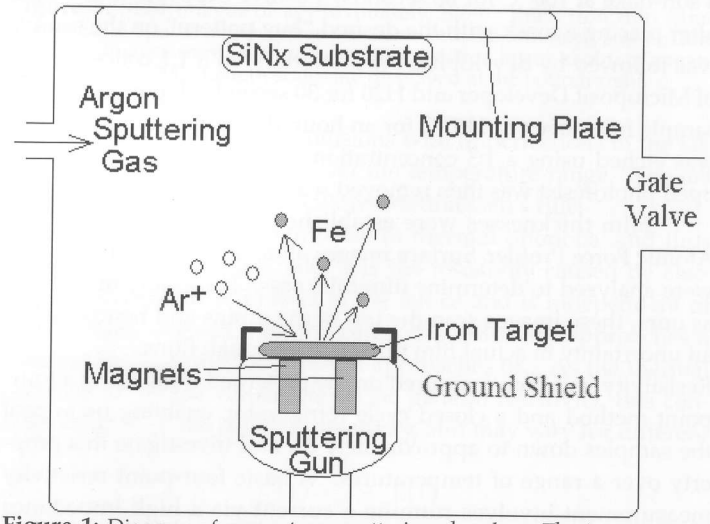

Figure 1: Diagram of magnetron sputtering chamber. The iron target is negatively biased. E&M field lines not shown.

Argon gas is then introduced into the chamber at a constant 25 sccm flow rate. Utilizing negative feedback, the main chamber gate valve adjusts the amount of gas being pumped back out, until the desired chamber pressure is attained. The iron target gun is

then powered by 150W DC, with a gun voltage of 420±10 V, and sputtering commences.

Argon atoms are ionized by a potential difference between the gun and the ground shield. These ions are accelerated towards the negatively biased iron target, thus ejecting iron atoms into the gas phase which then coat the chamber and in particular, the substrate. The argon ion/electron plasma is confined to the region near the gun by magnets behind the target. This increases the ionization efficiency, resulting in higher sputter rates, and allows sputtering at low argon gas pressures (~1mTorr).

Various factors determine the sputter rate, including the masses of the argon ions and iron atoms as well as the binding energy of the latter, all three of which are constants in our investigation. The energy of the incident ions, which can be varied by altering the target gun's bias voltage, and the argon gas pressure also affect the sputtering rate. Deposition rates were monitored via a quartz crystal rate detector.

The effect of film thickness on resistivity was examined. At a constant argon sputtering gas pressure of 2mTorr, four different thicknesses of iron, ranging from 160 _ to 2300 _, were grown on SiNx covered silicon substrates. The resistivity of these samples were then measured. Our primary investigation involved characterizing iron thin films deposited under the three different chamber pressures of 0.8mTorr, 2mTorr, and 8mTorr. All of these films were approximately 2000 _ thick and their electrical resistivity as well as magnetic properties were determined.

During each run, thin films were also deposited on 0.001" thick Kapton substrates. Film stress can be determined by measuring the resulting curvature of these substrates (Hellman et al. 1992).

Electrical Resistivity: A 1cm x 1cm sample of the deposited thin films was prepared for resistivity measurements by imprinting a well-defined geometry on the sample via photolithography. Photolithography involves spinning a thin layer of Shipley 1818 photoresist at 5000 rpm for 30 seconds on our sample followed by a soft-bake at 100° C for 60 seconds. Positive exposure to UV light after placing a mask with the desired "bug pattern" on the sample was followed by developing the photoresist in a 1:1 concentration of Microposit Developer and H20 for 30 seconds. Upon baking the sample in an oven at 115° C for an hour, the pattern on the sample was etched using a 1:5 concentration of HCl to H20. The developed photoresist was then removed with acetone.

Film thicknesses were established using a Nanopics 2100 Atomic Force Profiler. Surface images along a step edge in the film were analyzed to determine film thickness. For grainy films, such as ours, these images scan the top of the grains and hence lead to an uncertainty in actual film thickness for rough films.

Resistivity was then measured on the patterned films using a four-point method and a closed cycle refrigerator, enabling us to cool the samples down to approximately 3K and investigate this property over a range of temperatures. A basic four-point resistivity measurement involves running a current via a high impedance current source through two outer probes on the sample; voltage is measured across two inner probes, which do not draw current, and thus measure only the resistance of the sample and not of the probe itself. Cooling and heating runs revealed no hysteresis in sample resistivity.

Vibrating Sample Magnetometer (VSM): A clean, non-etched, 1cm x 0.5cm thin film sample is attached to the end of 50 cm quartz rod using Scotch double tape. The quartz rod is attach a vibrating head and an external applied magnetic field is duced by an electromagnet, which is a pair of coils with a core. The sample is positioned in the gap of the iron core, he a homogenous field. Pick up coils near the specimen experi change in magnetic flux due to the vibrating sample in th form applied field. By Faraday's law, if the electric wire ma turns in the inductor coil, an electromotive force, V, propor to the rate of change of that flux, , is induced in the pick up Compared to a signal produced by a standard nickel spher output signal is proportional to the magnetic moment of the ple. Samples were positioned both in-plane and out-of-pl the external field at room temperature. The applied external netic field was varied at a rate of 29.6 Gauss/s to produce a plete hysteresis loop between -9000 and 9000 Gauss. Backg measurements of just the rod and tape with a plain SiNx co silicon substrate (without iron) revealed a peculiar backg signal as large as 7% of the film's signal. This backgrou accounted for in our data and is most likely due to magneti in the environment.

Scanning Electron Microscope (SEM) and Energy Disp Spectrometer (EDS): A Hitachi analytical SEM was utilized t duce surface images and as an EDS. A clean, non-etched, th sample is mounted on a plate via carbon tape. Once loade face images at magnifications of up to 180K could be taken u 30 KeV electron beam. SEM showed top-down images of ple's surface, revealing grains whose sizes are measured.

In EDS, the incident electron beam excites atoms in th ple, which then eject x-rays whose energies vary depending the excitation states of the particular atom. EDS measures t

$$V = -N\frac{d\Phi}{dt}$$

quency of these x-rays and thus relative amounts of elemen sample can be determined. EDS done on our iron films rev contamination of the samples by argon. The film gr 0.8mTorr pressure had no oxygen, within its 0.30% margin o This implies that this sample hardly oxidized, if at all, when film grown at 8mTorr had 1.3 ± 0.2% oxygen. Oxygen co likely due to oxidation of the surface, including grain bou the rougher, larger grains of the 8mTorr sample allow more area over which an oxide layer can form. Samples were sto vacuum desiccator to minimize oxidation.

RESULTS AND DISCUSSION

The literature shows that sputtered thin films deposited pressures exhibit compressive stress while those sputtered a er chamber pressures have tensile stress (Thornton 1977 crossover pressure depends on the atomic mass of the targe rial. Film stress was quantitatively analyzed by measur radius of curvature of the thin films when grown onto a 0.001" Kapton substrate, the results presented in Figure 2. present case, all of the samples curved inward towards the film growth, indicating all the iron films are under tensil Tensile stress decreased as the film thickness increased, mo

due to defects nucleating in the films as they become thicker, enabling them to relieve stress. Figure 2 shows that the stress as a function of pressure first increases from 0.24±0.6 GPa to 1.4±0.1 GPa and then decreases to 0.36±0.5 GPa at 8mTorr, exhibiting a rise and gradual decline observed in other thin films (Hoffman 1982).SEM images revealed the grain structure of the films. Images of the samples grown at 0.8mTorr and 8mTorr are presented in Figure 3. The grains in the low pressure sample are shaped like elongated ellipsoids. This sample is visually much flatter and denser than the higher pressure sample. The grains here resemble cylinders or specks of rice and measure about 90±40 nm x 26±10 nm. The sample deposited at higher pressure has much larger grains, and a rougher, jagged surface. Grains are approximately 100±30 nm x 72±20 nm. There is also much larger variation in grain size and shape for this sample relative to the 0.8mTorr sample. Some of the grains are oblong and others resemble asymmet-

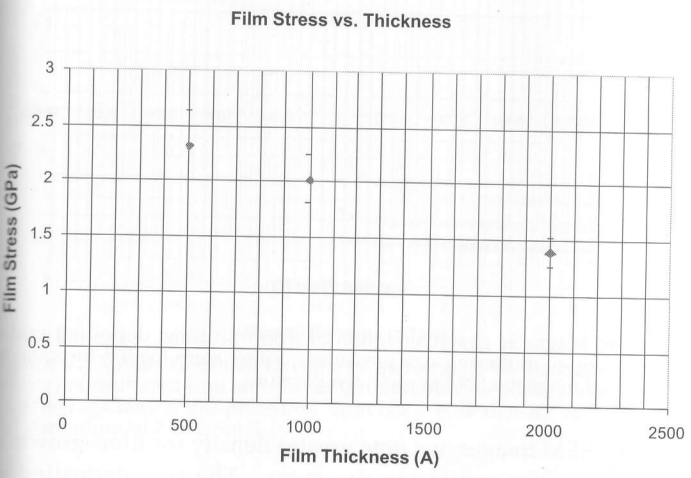

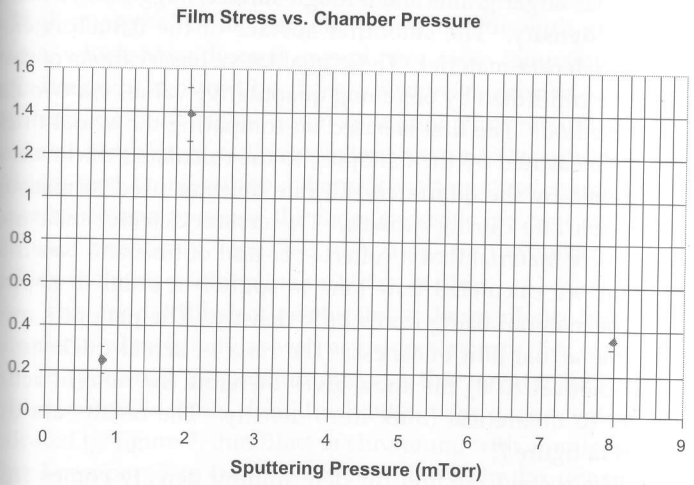

igure 2: Stress of iron thin films grown to different thicknesses (top) and nder various sputtering gas pressures (bottom).

ic stars or multi-pronged polyhedrons.

The effects of thickness and argon sputtering gas pressure n the electrical resistivity of the iron thin films are shown in figres 4 and 5. In varying sample thickness, the chamber pressure as set at a constant 2mTorr and the thicknesses ranged from 50_-2300_. The resistivity as a function of temperature is given in Figure 4. Note that at room temperature, the resistivity of bulk iron is 9.8 μ_·cm. The electrical resistivity of the metal films at room temperature (300K) is dominated by collisions of the conduction electrons with lattice phonons, which increase approximately linearly with temperature. At liquid helium temperature (4K), the

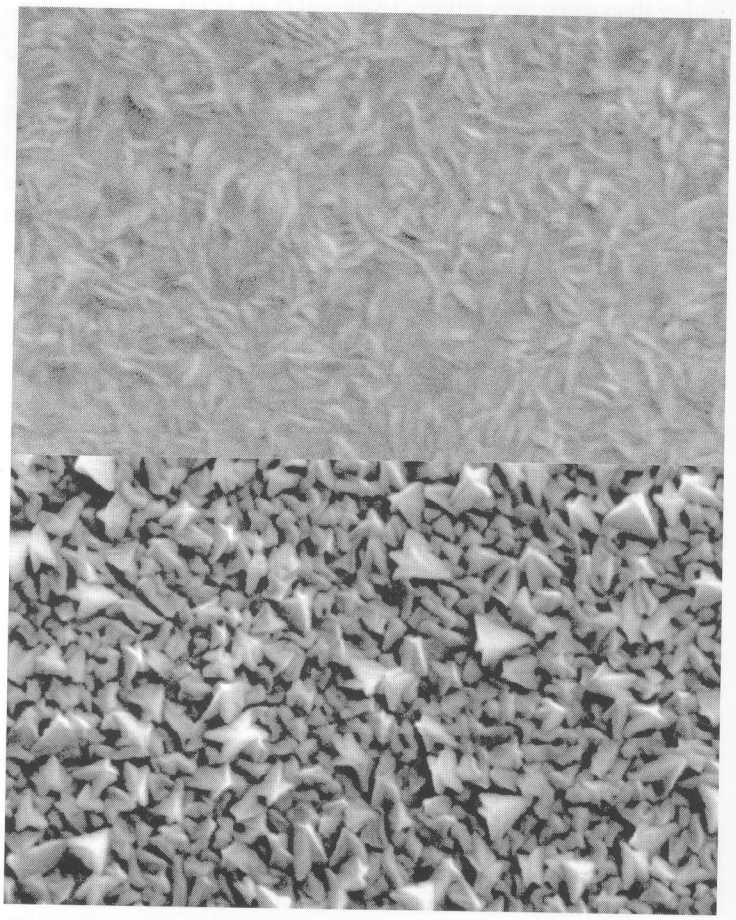

Figure 3: SEM images of approximately 2000 _ thick iron thin films deposited at sputtering chamber pressures of 0.8mTorr (top) and 8mTorr (bottom). Images were taken using a 30kV electron beam to obtain a magnification of 80,000. Length scales are displayed at the bottom right.

resistivity is dominated by collisions with imperfections in the lattice, which remain constant over the temperature range. The net resistivity in such materials follows Matthiessen's rule:
where _L(T) is the resistivity due to thermal phonons, and thus depends on temperature, and _i is the resistivity caused by electrons scattering off of defects in the lattice and is independent of temperature. As our data indicates, the resistivity approaches a constant value as the temperature approaches 0K. As the thermal phonons no longer contribute to the general resistivity, this constant value is _i, the residual resistivity, and may vary for different

$$(T) = \_i + \_L(T)$$

samples grown under the similar conditions. The greater residual resistivity of the 160 _ film can be attributed to the greater number of defects that perturb the periodicity of its lattice. The grain size must be smaller in the 160Å film since the thickness is significantly less than the grain size measured in the 2000_ films. Argon sputtering gas pressure strongly affects iron thin film resistivity. Sample resistivity as functions of temperature are plotted in figure 5.

The lattice resistivity, _L, should be the same for different specimens of a metal, as exemplified by the similar temperature dependence of the 0.8mTorr and 2mTorr thin films. The greater slope of the film grown at 8mTorr can be attributed to geometric factors, such as roughness of the film. This effect, studied in thin silver films, is most likely the result of the microstructure of the film rather than some new physics (Arnason et al. 1998).

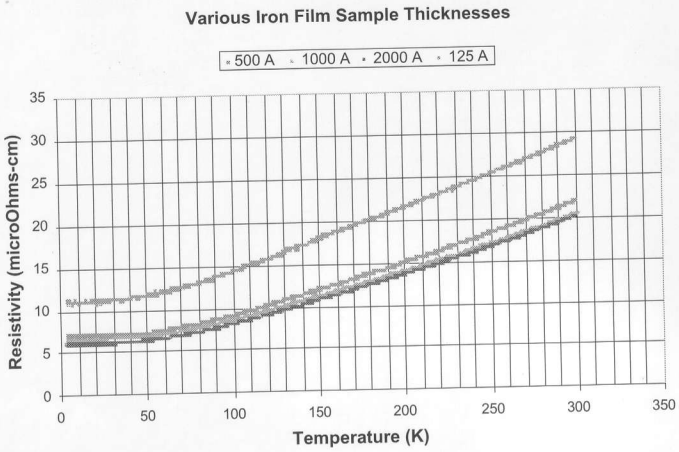

Figure 4: Resistivity of iron thin films grown to different thicknesses. Temperature ranges from approximately 2.6K up to 300K.

The magnetic characteristics of the films were examined at room temperature using a vibrating sample magnetometer. The films were placed such that the external magnetic field was either out-of-plane or in-plane. The results of the latter investigation are displayed in figure 6 after the background signal was subtracted. Bulk iron is known to be ferromagnetic. The magnetization of all of our films increases as the external applied field does until they reach a maximum moment. If the field is decreased from its value at the point where the change in the rate of magnetization begins to decrease, i.e. the inflection point, then the film's magnetization decreases along a different path and is slightly positive if the external field is completely removed. This hysteresis of our thin films is characteristic of ferromagnetic materials. Figure 6 shows that the saturation magnetization depends on sputtering gas pressure. Bulk iron saturates at 1714 emu/cc at room temperature (Cullity 1972). The 0.8mTorr thin film is similar, saturating at 1800 ± 140 emu/cc, but the samples grown at 2mTorr and 8mTorr have lower saturation magnetizations of 1570 ± 130 emu/cc and 1200 ± 100 emu/cc respectively. The films grown at higher pressures, as SEM images and subsequent density measurements indicate, are less dense than bulk iron and thus fewer atoms contribute to the magnetic moment per cubic centimeter of material.

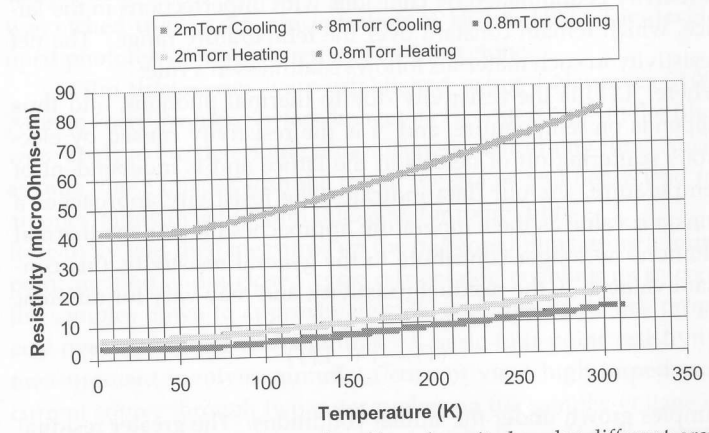

Figure 5: Resistivity of iron thin films deposited under different argon sputtering gas pressures. Temperature ranges from approximately 2.6K up to 300K.

The structure and densities of the films are important in understanding the electrical and magnetic properties observed.

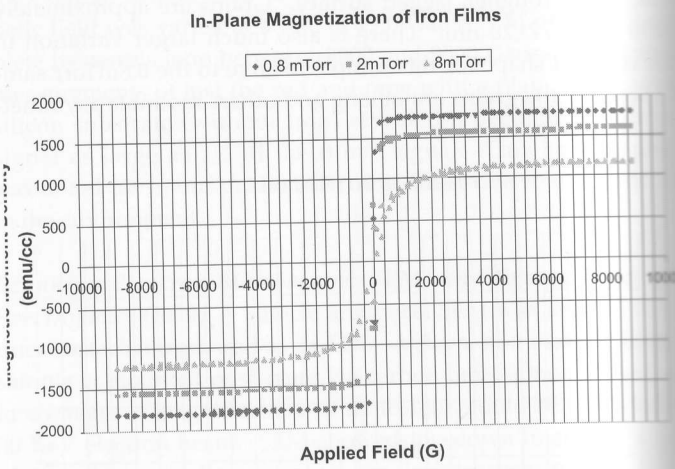

Figure 6: Magnetic characterization of iron thin films deposited under different argon sputtering gas pressures. Films were loaded in-plane to the external magnetic field at room temperature.

From the SEM images, we note greater density for films grown at lower argon gas sputtering pressures. The film deposited at 8mTorr has larger grains and a rough surface, suggesting a lower average density. The smoother surface of the 0.8mTorr film implies a denser material. These qualitative observations of density were confirmed by obtaining quantitative values via two different methods. The first is based on comparing the actual thickness, as measured by the nanopics, to the calculated thickness as determined by the quartz crystal rate detector used to measure deposition rate during growth. The crystal detector measures the mass of material that it collects per unit of time and based on this rate, we calculated how long to sputter in order to deposit 2000_ of material using iron's bulk density. The nanopics measures the actual film thickness. The ratio of actual thickness to the theoretical 2000_ thickness gives therefore the ratio of actual density to theoretical (bulk iron) density. The results are displayed in figure 7.

The second method for determining density comes from analyzing the in-plane magnetization curves. The saturation magnetization depends on how many atoms there are in a cubic centimeter since each atom contributes a magnetic moment. In comparing the saturation magnetization of our films to that of bulk iron, which at room temperature is 1714 emu/cc, we are able to

determine the ratio of the atomic density of our thin films compared to bulk iron. The results are displayed in figure 7 alongside the density of bulk iron. Both of these methods verify less dense films at higher sputtering pressures and reveal similar densities at respective pressures. Fundamentally, the structure of the films varies when deposited under different argon sputtering gas pressures. At higher pressures, the films are less dense and grains are much larger with more surface area. Such loose and voided grain boundaries impede the conduction of electricity, and hence result in greater resistivity for such films. This differs from the more tightly packed grains of the iron films grown at lower pressures with more contact between adjacent grains. Similar relations between sputtering chamber pressure and resistivity have been observed for Cr, Ti, Ni, Mo, and Ta thin films (Thorton et al. 1977). The varying densities of films can be understood in light of the

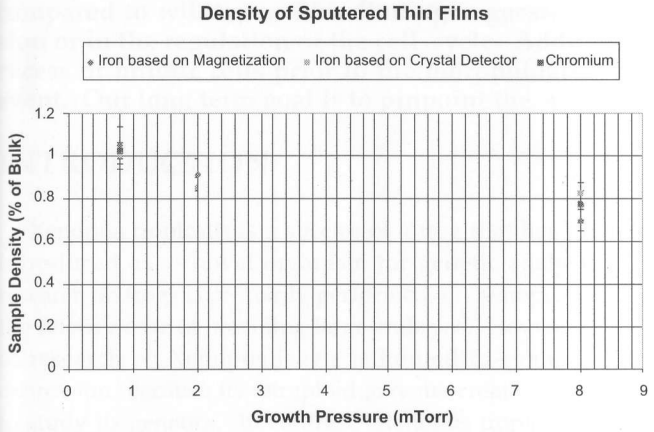

Figure 7: Atomic densities (given as a percentage of the bulk sample's density) of sputtered iron and chromium thin films deposited under different argon sputtering gas pressures. Iron has a bulk density of 7.87 g/cm3 and chromium of 7.19 g/cm3.

process of deposition. Target iron atoms are ejected by argon ions at high energy. These energetic atoms collide with argon gas atoms, which have thermal energy near room temperature, and their energy is reduced by these collisions, a process known as thermalization. At higher argon sputtering gas pressure, the iron atoms undergo more collisions before reaching the substrate. The incident iron atoms at the substrate are thus less energetic. At lower sputtering pressure, the more energetic incident atoms collide with previously deposited iron atoms on the substrate, thus packing them in, resulting in much denser films.

This model illustrating the dependence of structure, and thus electrical resistivity as well as magnetic properties of the thin film, on sputtering gas pressure suggests that target materials with similar atomic weights should exhibit similar dependencies. As indicated by figure 7, thin films of chromium, with atomic mass 52 g/mol compared to iron's 56 g/mol, have similar densities to those of iron thin films when grown at the same sputtering gas pressures. The resistivity of the chromium thin films, however, changes much more drastically when deposited under different chamber pressures, as displayed in figure 8 (Boekelheide 2006). Whereas the room temperature resistivity of the iron films grown at 8mTorr were never greater than 8 times those grown at 0.8mTorr, chromium thin films deposited at these pressures exhibit a 17 fold increase in resistivity. Furthermore, the sheer magnitudes of the chromium films' residual resistivity are greater; for example, the chromium film grown at 8 mTorr has a residual resistivity of 400 __-cm compared to iron's 40 __-cm. The conductivity of a metal, according to Boltzmann transport theory, is given by:

$$\sigma = \frac{e^2}{12\pi^3 \mathrm{h}} \tau(\varepsilon_F) \bar{v} S$$

where τ is the average scattering time, ε_F the Fermi energy, $\bar{v}$ the average velocity at the Fermi surface, and S the k-space area of the Fermi surface. (Ashcroft et al. 259). Loose grain boundaries, like those observed in the iron films grown at higher sputtering pressures, decrease the average scattering time _ and hence increase the resistivity of the material. SEM images of chromium thin films reveal similar larger, loose grain boundaries, when deposited at

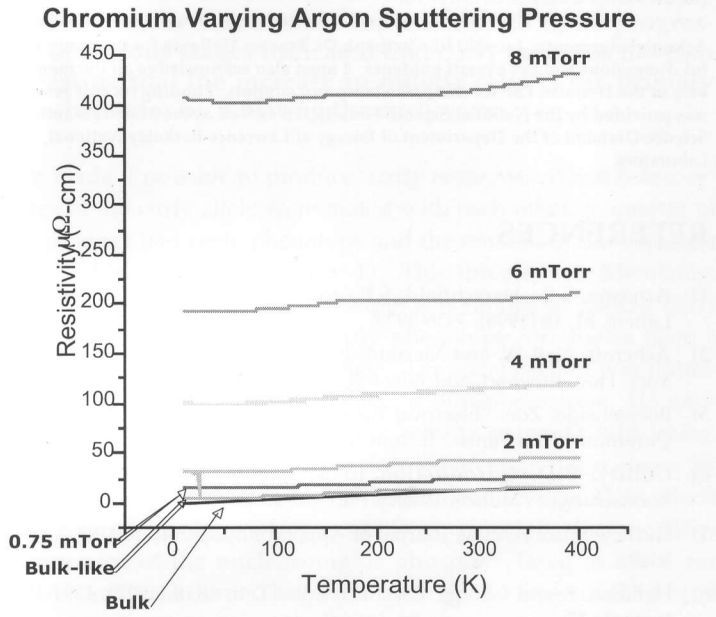

Figure 8: Resistivity of chromium thin films deposited under different argon sputtering gas pressures. Courtesy of Z. Boekelheide.

higher chamber pressures (Boekelheide 2006). These films, with greater voids, were also found to be less dense than those grown at lower sputtering pressures. Structural variations, as our data for iron suggests, are not sufficient to explain the extensive variation of resistivity observed in chromium thin films. The antiferromagnetic chromium, unlike iron, possesses an incommensurate spin density wave which has been shown to be sensitive to film thickness effects (Rotenberg 2005). Deviations in band structure of the chromium films could change the sensitivity of the average velocity at the Fermi surface, on growth pressure and S, the k-space area of the Fermi surface. Indeed, recent examinations of chromium reveal a shift from commensurate spin density waves in thin films grown at sputtering pressures below 2mTorr to a suppressed spin density wave in films deposited at higher pressures (Boekelheide 2006).

CONCLUSION

Investigations of sputtered iron thin films reveal a dependence of their electric and magnetic properties on deposition conditions. Films of various thicknesses exhibited less stress in thicker films

resulting from microstructural changes. Films deposited at higher argon sputtering gas pressures possess larger grains in a rougher surface. The greater voids in these films result in less dense materials and higher resistivity than those deposited at lower chamber pressures. Magnetization measurements confirm the correlation between deposition pressure and film density. Comparisons to chromium thin films reveal similar structural properties so drastically larger resistivity in the latter suggest band effects at work in Cr thin films.

Currently, various compositions of Fe-Cr alloys are being investigated. The juxtaposition of the ferromagnetic iron and chromium, with its assortment of spin density wave regimes, can be comprehended once the dependence on deposition conditions of thin films of iron and chromium separately are understood. Subsequent research will focus on the effects of deposition parameters on Fe/Cr multilayers.

Acknowledgements: I would like to thank Dr. Frances Hellman for the many fruitful discussions and her overall guidance. I must also acknowledge all the members of the Hellman Lab for their assistance and support. Funding for this research was provided by the National Science Foundation as well as the Materials and Science Division of the Department of Energy at Lawrence Berkeley National Laboratory.

REFERENCES

1) Arnason, S.B., Herschfield, S.P., and Hebard, A.F. Physical Review Letters. 81, 18 (1998), 3936-3939.
2) Ashcroft, Neil W. and Mermin, N. David, Solid State Physics, New York: Holt, Rinehart, and Winston, 1976. pg. 259.
3) Boekelheide, Zoe. "Electrical Resistivity and Reflectivity of Sputtered Chromium Thin Films." Technical Report (2006).
4) Cullity, B.D. Introduction to Magnetic Materials. Reading, Massachusets: Addison-Wesley Pub. Co. 1972.
5) Gurney, Bruce A. et al, Journal of Applied Physics. 70, 10 (1991), 5867-5869.
6) Hellman, F. and Gyorgy, E.M., Phys. Rev.Lett. 68, 9 (1992), 1391-1394, footnote 25.
7) Hoffman, D.W. and Thornton, John A. J. Vac. Sci. Technol., 20, 3 (1982), 355-358.
8) Kittel, Charles. Introduction to Solid State Physics. 8th Edition. John Wiley & Sons, Inc. 2005.
9) Thornton, John A and Hoffman, David W. J. Vac. Sci. Technol., 14, 1 (1977), 164-168.
10) Rotenberg, E. et al, New Journal of Physics 7 (2005).